Taylor & Francis
Taylor & Francis Group

Artificial Cells, Nanomedicine, and Biotechnology

An International Journal

ISSN: 2169-1401 (Print) 2169-141X (Online) Journal homepage: https://www.tandfonline.com/loi/ianb20

NIR triggered glycosylated gold nanoshell as a photothermal agent on melanoma cancer cells

Samira Nouri, Elham Mohammadi, Bita Mehravi, Fatemehsadat Majidi, Khadijeh Ashtari, Ali Neshasteh-Riz & Samira Einali

To cite this article: Samira Nouri, Elham Mohammadi, Bita Mehravi, Fatemehsadat Majidi, Khadijeh Ashtari, Ali Neshasteh-Riz & Samira Einali (2019) NIR triggered glycosylated gold nanoshell as a photothermal agent on melanoma cancer cells, Artificial Cells, Nanomedicine, and Biotechnology, 47:1, 2316-2324, DOI: 10.1080/21691401.2019.1593187

To link to this article: https://doi.org/10.1080/21691401.2019.1593187

Published online: 11 Jun 2019.

ARTIFICIAL CELLS, NANOMEDICINE, AND BIOTECHNOLOGY
2019, VOL. 47, NO. 1, 2316–2324
https://doi.org/10.1080/21691401.2019.1593187

NIR triggered glycosylated gold nanoshell as a photothermal agent on melanoma cancer cells

Samira Nouri[a,c], Elham Mohammadi[b], Bita Mehravi[b], Fatemehsadat Majidi[a,c], Khadijeh Ashtari[b], Ali Neshasteh-Riz[a]* and Samira Einali[a]

[a]Radiation Biology Research Center, Iran University of Medical Sciences, Tehran, Iran; [b]Department of Medical Nanotechnologies, Faculty of Medical Nanotechnology, University of Medical Sciences, Tehran, Iran; [c]Cellular and Molecular Research Center, Iran University of Medical Sciences, Tehran, Iran

ABSTRACT

Nowadays, gold nanoshells are used in targeted nano photothermal cancer therapy. This study surveyed the application of gold nanoshell (GNs) to thermal ablative therapy for melanoma cancer cells and it takes advantage of the near infrared absorption of gold nanoshells. The synthesis and characterization of glycosylated gold nanoshells (GGNs) were done. The cytotoxicity and photothermal effects of GNs on melanoma cells were evaluated using MTT assay and flow cytometry. The characterization data showed that GGNs are spherical, with a hydrodynamic size of 46.7 nm. Results suggest that the cellular uptake of GGNs was about 78%. Viability assays showed no significant toxicity at low concentrations of GNs. The higher heating rate and toxicity of cancer cells were obtained for the cells exposed to 808 nm NIR laser after incubation with GGNs rather than the GNs. The viability of these cells has dramatically decreased by 29%. Furthermore, 61% more cell lethality was achieved for A375 cells using combined photothermal therapy and treatment with GGNs in comparison to NIR radiation alone. In conclusion, our findings suggest that the synthesized gold/silica core-shell nanoparticles conjugated with glucosamine have high potentials to be considered as an efficient metal-nanoshell in the process of targeted cancer photothermal therapy.

ARTICLE HISTORY
Received 24 November 2018
Revised 30 January 2019
Accepted 30 January 2019

KEYWORDS
Cellular uptake; gold nanoshells; glucosamine; melanoma cancer; NIR; photothermal therapy

Introduction

Malignant melanoma is the most aggressive form of skin cancer. Early-stage melanoma can be removed by surgery [1]. The tumour excision is a standard effective therapeutic method of cancer treatment. However, it is not an efficient method particularly when the cancerous cells metastasize to other organs [2]. Therefore, metastasized melanoma cells should be treated via other therapies such as chemotherapy, radiotherapy, targeted therapy and hyperthermia [1].

Conventional hyperthermia is used to kill the cancerous cells and is considered as an invasive method of treatment for different kinds of cancer. Knowing that the cancer cells are more susceptible to heat than healthy cells, hyperthermia can kill tumour cells at temperatures above 40 °C. However, hyperthermia is not able to treat cancer cells without damaging the adjacent tissues [2].

Recently, photothermal therapy has drawn great attention as a supplementary method compared to traditional cancer treatment. Photothermal therapy uses photothermal agents which convert light energy to heat. Eventually, it results in elevated cell temperature, thereby ablating cancer cells effectively without damaging the adjacent normal cells [3–5]. Among the various light sources, the light near infra-red (NIR) rang 700–1000 nm is particularly suitable because of low scattering and low absorption by blood and by soft tissue cells in this spectral region [6,7]. Photothermal agents have a strong absorbance in the NIR region to convert light energy to heat locally [5–7].

Today, nanostructures such as nanorods [3], polymers [4], mesoporouse silica nanoparticles [8], nanoshells [9], nanocomposites [8], magnetic nanoparticles [10], nanostars [11] and dendrimers [12,13] are used extensively in medical applications especially cancer imaging and therapy. Gold nanoparticles seem to be an extraordinary candidate for medical applications due to their low toxicity [11,14], stability, easy synthesis and surface modification [11].

Gold nanoshells usually consist of a dielectric core such as silica encapsulated by a thin Au layer [9,14]. The unique optical feature of gold nanoshells is attributed to the surface plasmon resonance (SPR) of gold metal electrons. This feature can be improved by controlling the size, thickness and other parameters of the gold shell during the synthesis processes

CONTACT Bita Mehravi mehravi.b@iums.ac.ir Department of Medical Nanotechnologies, Faculty of Medical Nanotechnology, University of Medical Sciences, Tehran 14496, Iran.
*Co-corresponding author.
This article has been republished with minor changes. These changes do not impact the academic content of the article.

[14]. Gold nanoshells, as a photothermal agent, can significantly convert the absorbed light energy to localized heat by surface plasmon resonance (SPR) in the NIR region. They cause irreversible damage to cancer cells while preventing damage to normal cells which are adjacent to them [14,15].

Silica is a necessary component of human body. It is nontoxic, biocompatible and biodegradable in relation to liposomes and dendrimers [16,17]. It can also disperse freely throughout the whole body and be excreted in the urine [16]. The high level of silanel groups in silica increases its affinity to phospholipids, so it can be easily taken up by cells [17].

Conjugation of groups which target the surface of nanoparticles can be applied for enhancing the permeability and retention of nanoparticles to cancer cells. Different groups have been developed to target nanoparticles and incorporate them into cells. Glucose is one of these groups for targeting cancer cells which have an excessive demand for glucose. This requirement is met through enhancing cellular uptake of glucose by particular transporters [18–20]. The glucose transporter-1 (Glut-1) is a membrane protein which facilitates the intra-cellular uptake of glucose. The overexpression of Glut-1 is associated with high glucose transfer to cancer cells [19,20]. Accumulation of glucose in the tumour cells is very high because of their high rate of proliferation and angiogenesis [18]. This property can also be employed for cancer treatment. For enhancing the potential localized photothermal therapy, glucosamine can be conjugated to GNs surfaces. This modification improves internalization and accumulation of GNs in the cells. Subsequently, the effects of photothermal therapy can increase considerably while reducing its side effects [2,9,14,21,22].

A unique targeting based on glucose-modified GNs was designed and synthesized which is called GGNs. They are able to target and kill melanoma cancer cells under 808 nm NIR laser irradiation (Figure 1). The cytotoxicity of GGNs was assessed using MTT assay. The results indicated that GGNs have an antitumor effect on melanoma cancer cells. MTT assay and Flow cytometry approved that GGNs are great photothermal agents because of surface plasmon resonance in NIR region, thereby killing melanoma cancer cells.

Materials and methods

Materials

Hydrogen tetrachloroaurate hydrate (III) ($HAuCl_4$, $3H_2O$, 99.99%, AlfaAesar), sodium hydroxide (NaOH, Sigma-Aldrich), ammonium hydroxide (NH_4OH), potassium carbonate (K_2CO_3, AR Grade), sodium borohydride ($NaBH_4$), 3-aminopropyl-triethoxysilane (APTES, 99%, Sigma-Aldrich), tetraethyl orthosilicate (TEOS, 98%), anhydrous ethanol (EtOH, 99.5%), glucose amine, bicarbonate (H_2CO_3), mercaptoecanoic acid, N-hydoxysulfosuccin imide (NHS) and dimethylaminopropyl carbod imide (EDC) were provided from Acros Co. (Belgium) and used without further purification. The dubleccos Modified Eagles Medium (DMEM) high glucose and low glucose, fetal bovine serum (FBS), penicillin/streptomycin, Annexin V-FITC and propidine Iodide (PI) were purchased from Sigma Aldrich. Finally, 3–(4,5-dimethylthiazol-2-yl)-2,5-diphenyltetrazolium bromide (MTT) and Dimethyl sulfoxide (DMSO) were provided by Tarbiat Modares University (Tehran, Iran).

Preparation of monodispersed silica nanoparticles

To prepare SiO_2 nanoparticles, TEOS was hydrolyzed in ethanol by deionized water in the presence of ammonium hydroxide, according to Stöber et al [23]. The volume ratio of TEOS: ETOH: H_2O: NH_4OH was (1.5:20.0:0.8:7.2 ml). This solution was stirred for 30 min vigorously until a white turbid suspension was obtained. The solution of nanoparticles was then centrifuged (at 10,000 rpm for 20 min). Finally, the separated nanoparticles were washed by deionized water and ethanol twice.

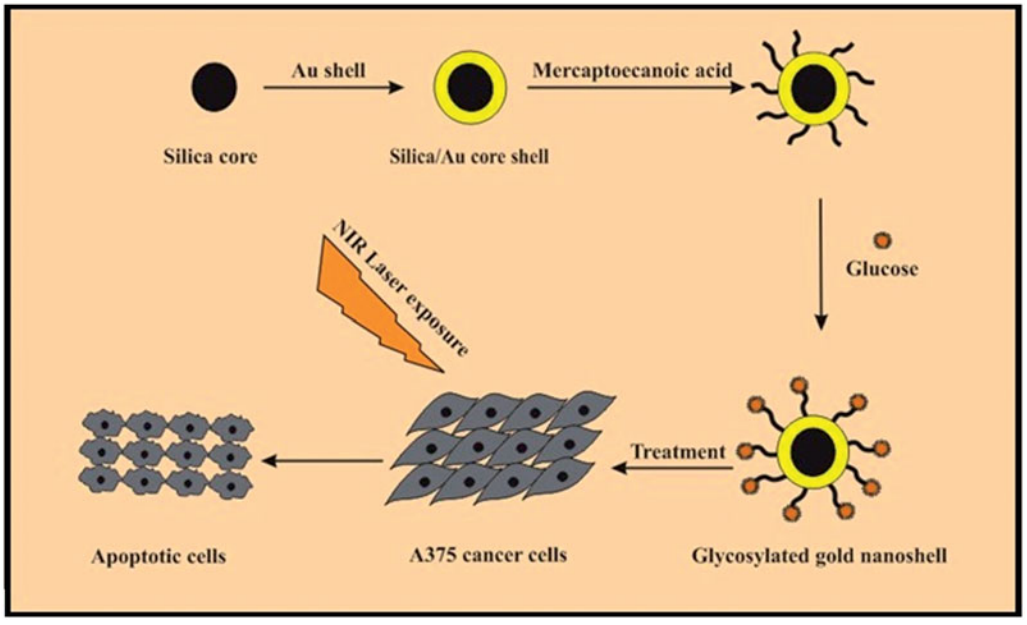

Figure 1. A schematic description for synthesis a glycosylated gold nanoshell and photothermal ablation of melanoma cells under NIR laser irradiation.

Grafting APTES on silica nanoparticles

To obtain APTES-grafted silica nanoparticles, APTES was added to the silica nanoparticles at a 2:1 weight ratio. Then, the solution was stirred at room temperature for 24 h. APTES-grafted silica was separated through centrifugation (at 10,000 rpm for 10 min), and the product was washed with deionized water and ethanol.

Gold seeding on APTES-Grafted silica nanoparticles

First, 0.06 g $HAuCl_4.3H_2o$ was dissolved in 25 ml of deionized water and then was added into APTES-grafted silica nanoparticles. The solution pH was adjusted to 7 by adding 0.1 M of NaOH. It was then stirred in an oil bath at 70 °C for 2 h. The product was separated via centrifugation (at 15,000 rpm within 10 min) and washed with deionized water and ethanol twice. Eventually, the product was dispersed by ultrasonication in 10 ml of water.

Preparation of gold nanoshells

Gold-K aqueous solution was synthesized by mixing 280 mg/l K_2CO_3 powder with 250 ml deionized water. Next, 2 ml of 25 ml solution of $HAuCl_4$ was prepared. Finally, Au.K and Au-seeded silica were mixed together with a 500:1 volume ratio.

Conjugation of glucosamine on gold nanoshells

To prepare functionalized nanoparticles with glucose, first, the amine group of glucosamine should have been activated by adding H_2CO_3 to 2 ml of aqueous solution of glucosamine. It was then mixed with nanoparticles linked to 10^{-3} M of mercaptoecanoic acid as a linker. NHS and EDC were further added to this solution. The mixed solution was stirred for 1–2 h at room temperature. The mixed solution was separated by centrifugation and was washed three times with deionized water and ethanol to remove the excess reagents. The synthesis procedures of GNs and GGNs are illustrated in Figure 2.

Characterization

Scanning electron microscopy (SEM) was utilized to evaluate the morphology and size of GGNs (SEM, philips 97, XL-30, Holland).

Dynamic light scattering (DLS) was used to study the size of gold nanoparticles. This rapid method is used to determine the particle size within the range of a few nanometers to micron (Nanoflex zeta sizer, Germany).

Fourier transform-infrared (FT-IR) spectroscopy is an analytical technique which identifies chemical bonds in gold nanoparticles by generating an infrared absorption spectrum. FT-IR was used to confirm the existence of the linker and glucose on the surface of GNs within the region of 400–4000 cm^{-1} (FTIR spectrophotometer, PerkinElimer, Frontier, USA).

UV-visible spectroscopy is a method for measuring the light which is absorbed by gold nanoparticles. The peak of absorption in the UV-visible spectrum depends on the size, shape, and compounds of gold nanoparticles (UV-visible spectrophotometer, Pharmacia Biotech, Germany) [24].

Cell culture

Melanoma (A375) and human dermal fibroblast (HDF) cell lines were bought from Pasteur Institute, Tehran, Iran. A375 cell lines were maintained in DMEM high glucose containing 10% Fetal Bovine Serum (FBS) and 1% penicillin/streptomycin. HDF cell lines were grown in DMEM low glucose supplemented with 10% FBS and 1% penicillin/streptomycin. All cells were incubated at 37 °C and CO_2 5% environment.

Intra-cellular uptake of GGNs

For detecting intra-cellular uptake of GGNs and GNs, A375 and HDF cell lines were placed in six-well plates (2×10^6 cells per well) and incubated at 37 °C and CO_2 5% for 24 h. GGNs (100 μg/ml) were then added to each well. The cells were incubated for 2 h and washed twice with PBS. Next, they were centrifuged at 1000 rpm for 4 min and suspended in

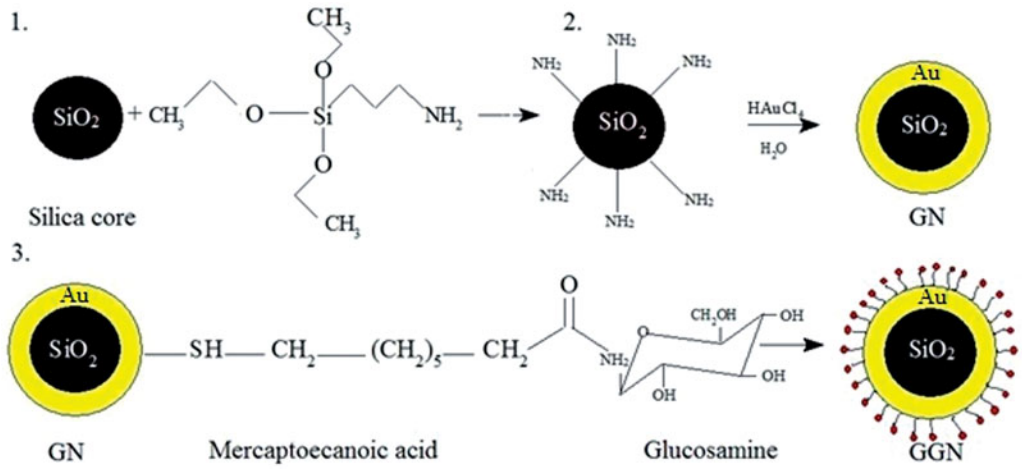

Figure 2. Schematic illustration of synthesis procedure of GNs and GGNs.

100 µl of PBS. The intra-cellular uptake of GGNs was determined using ICP-AES (perkin Elmer Optima, 3100XL).

Cytotoxicity assay

The cytotoxicity of GGNs on A375 and HDF cell lines was assessed using MTT assay. A375 and HDF cell lines were seeded into 96-well plates (1×10^4 cells per well) containing DMEM at 37 °C and CO_2 5% to be attached overnight. The medium was replaced with a fresh medium containing various concentrations of GGNs. Then, after 24 h of incubation, the medium was removed and the cells were washed by PBS, and MTT solution (5 mg ml^{-1}PBS) was added in each well. After 4 h of incubation, formazan crystals were dissolved in 100 µl of DMSO within 15 min of incubation. Finally, the absorbance of each well was measured at 570 nm by a micro plate reader [2] (Micro plate reader, 68, Japan).

Photothermal effects of GGNs on melanoma cancer cells

A375 cells were subcultured in 96-well plates (1×10^4 cells per well) for 24 h. Then, the cells were incubated with GNs and GGNs 50 µg/ml for 4 h. Next, the cells were exposed to 808 nm NIR laser with a power of 0.9 Wcm^{-2} for different times (LT-IR, USA). Thereafter, they were incubated at 37 °C with CO_2 5% for 24 h. Eventually, the MTT assay was performed to measure the cell viability.

Assessing cell apoptosis

Apoptosis and necrosis were examined on A375 cells in six samples including the control, GNs, GGNs, laser, laser after GNs treatment, and GGNs treatment by flow cytometry. A375 cells were seeded into 48-well plates (1×10^5 cell per well), then were incubated with GNs and GGNs for 4 h. After washing, the cells were exposed to NIR laser for 1 min and then returned to the 37 °C incubator for 24 h. Subsequently, the cells were washed with PBS and then suspended in 1 ml PBS, 100 µl of the solution was transferred to 5 ml tube, and 5 µl of Annexin V-FITC and 5 µl of PI were added and incubated in a dark place for 15 min. Finally, the labelled cells were analyzed by a flow cytometer [25] (BD FACS Calibur, San Jose, CA, USA).

Statistical analysis

Multi-group comparison of the means was evaluated using one-way ANOVA test, whereas two-group comparison of the means was analyzed using *t*-test. The statistical significance difference for cell toxicity and photothermal effects was set at $p < .05$. All experiments were replicated three times ($n = 3$).

Results

Synthesis of glycosylated gold nanoshells

APTES was used to add amino groups to the silica core. After the reaction of Au and silica nanoparticles, gold nanoshells were washed to remove excess APTES and Au which did not participate in the reaction, when finally a reddish solution was observed. The glucosamine as a macromolecule and monosaccharide family was conjugated to GNs with the aim of targeting melanoma cancer cells. To conjugate glucose, first, amine groups of glucosamine should be activated. The free electrons of the amine attack to the carbonyle groups of mercaptoecanoic acid which was used as a linker.

Characterization of glycosylate GNs

SEM was applied to evaluate the appearance and size of GGNs. Figure 3 displays that GGNs have a spherical morphology and an average diameter of 40 nm. DLS was used to measure the size of GGNs. Figure 4 indicates that the GGNs have 47.6 nm diameter.

FT-IR spectroscopy was conducted to confirm the existence of functional groups on GNs within the region of 400–4000 cm^{-1}. Figure 5 confirms that the linker and glucose have been bound.

UV-visible spectroscope was applied to measure the light absorption of GGNs. Figure 6 shows that the peak absorption of GGNs is around 808 nm.

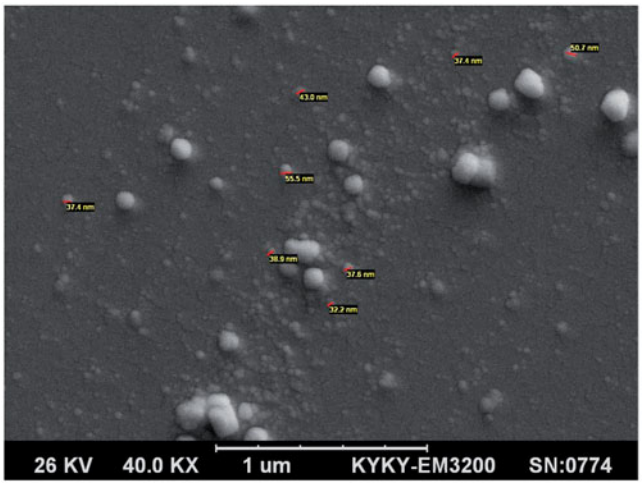

Figure 3. SEM image of GGNs.

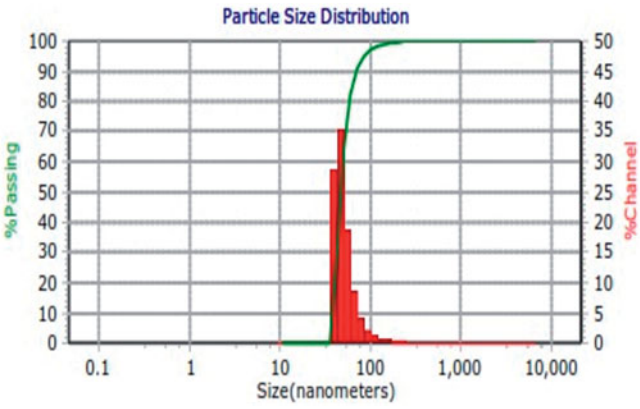

Figure 4. DLS measurment of size distribution of GGNs.

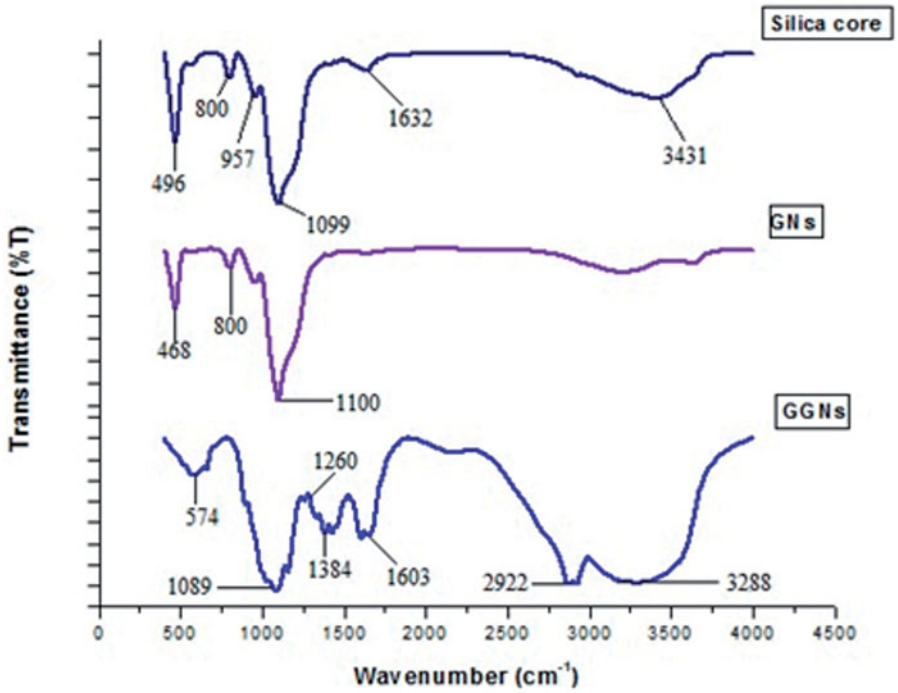

Figure 5. FT-IR spectra of silica core, GNs and GGNs.

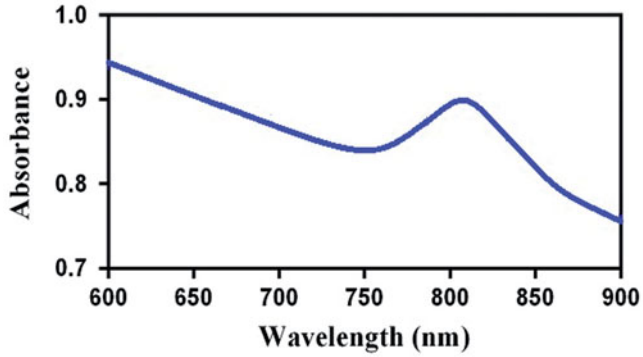

Figure 6. UV.visible spectrum of GGNs.

Intra-cellular uptake of GGNs

Figure 7(a) displays the intra-cellular uptake of GGNs into A375 cancer cells, where the percentage of GNs and GGNs in cells was 11.35% and 77.67%, respectively. To assess the "in-vitro" capability of the GGNs to discriminate between normal and cancer cells, an ICP-AES analysis was performed on HDF and A375 cell lines. Figure 7(b) reveals that GGNs intra-cellular uptake in HDF cells was 3%. Further, human melanoma cancer cell (A375 cells) was higher than that found in human normal fibroblast (HDF) cells.

Cell viability

The results demonstrated cytotoxicity of GNs and GGNs with regards to the concentration of GNs. GNs and GGNs showed insignificant cytotoxicity to HDF cells when the concentration of GGNs was lower than 200 μg/ml. By increasing the concentration, cytotoxicity was elevated significantly. When the concentration of GNs and GGNs was 400 μg/ml, the viability of HDF cells was 58% and 54%, respectively (Figure 8(a)).

Great antitumor effect of GGNs was revealed in A375 cells with overexpression glucose transporter compared to HDF cells. The cell viability decreased dramatically with increasing of GGNs concentration. There is a clear difference between the cytotoxic effect of GNs and GGNs. At GNs and GGNs 50 μg/ml, the cell viability was 77% and 56%, respectively (Figure 8(b)).

The effect of photothermal therapy

To investigate the effect of photothermal therapy, A375 cells were incubated with GNs and GGNs 50 μg/ml for 4 h. Then, the cells were treated with 808 nm NIR laser for several times. Finally, MTT assay was performed to assess the cell viability.

The results indicated that the viability of A375 cells exposed to NIR laser after incubation with GNs and GGNs decreased significantly by increasing the exposure time. The cell viability of the GGNs incubating A375 cells was significantly lower than the viability of A375 cells incubated with GNs. When 1 min was selected as the exposure time, the cell viability of the A375 cells which were incubated by GNs and GGNs was 64% and 29%, respectively (Figure 9).

Flow cytometry was utilized to evaluate the apoptosis of A375 cells treated using NIR laser after incubation by GGNs. A double-staining flow cytometry included two dyes including Annexin V-FITC and PI. Annexin V-FTIC can react with live cells, whereas PI is used to indicate apoptotic and necrotic cells [26]. Figure 10(a) reveals the percentages of A375 cells viability (A^-/PI^-), early apoptosis (A^-/PI^+), late apoptosis (A^+/PI^+) and necrosis (A^-/PI^+) in six samples as mentioned previously.

The photothermal effect was proved by flow cytometry. Figure 10(b) illustrates the percentage of apoptotic cells.

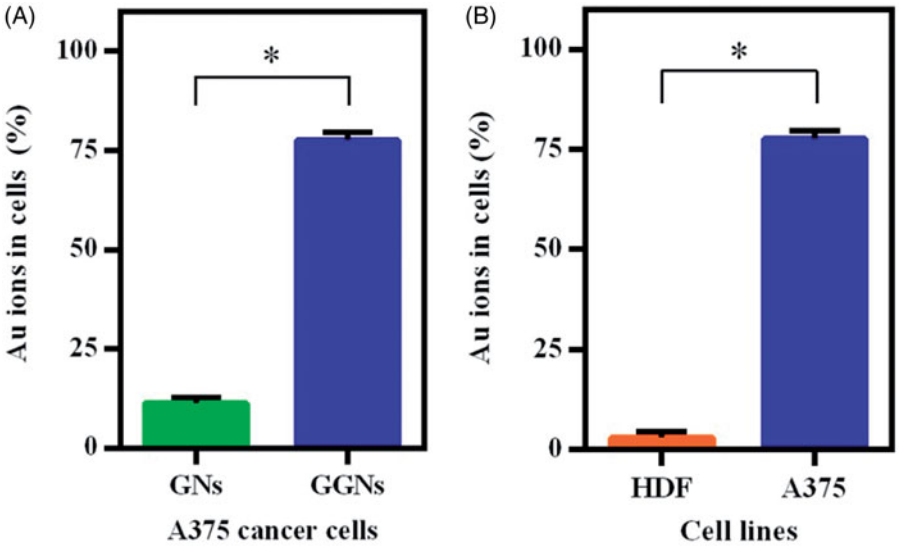

Figure 7. Intra-cellular uptake assay of GNs and GGNs. (a) Compare the uptake of GNs and GGNs in A375 cancer cells. (b) Indicate the difference of uptake of GGNs in HDF and A375 cell lines.

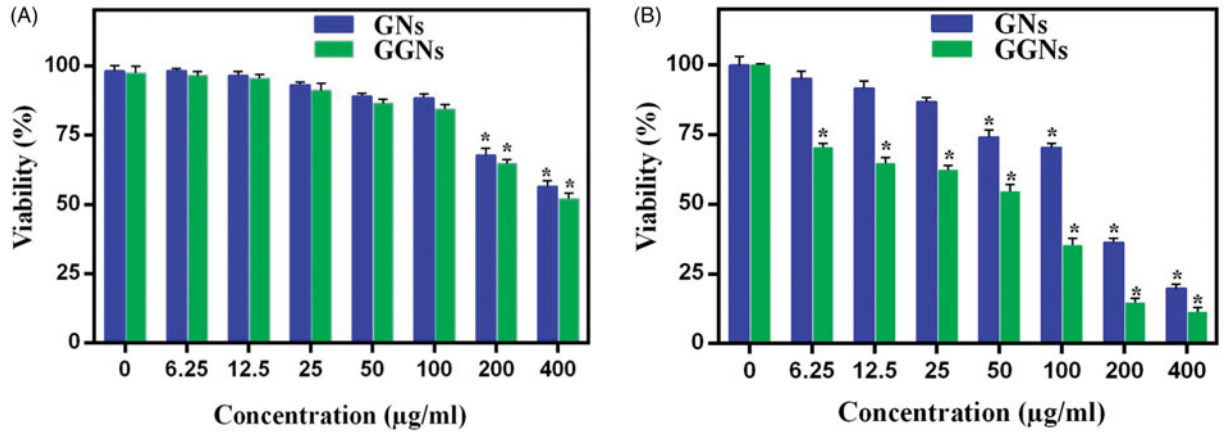

Figure 8. Cell viabilites of the (a) HDF and (b) A375 cells incubated by various concentration of GNs and GGNs for 24 h. All data represent average value of triplicate.*p Values $< .05$, compared with control group.

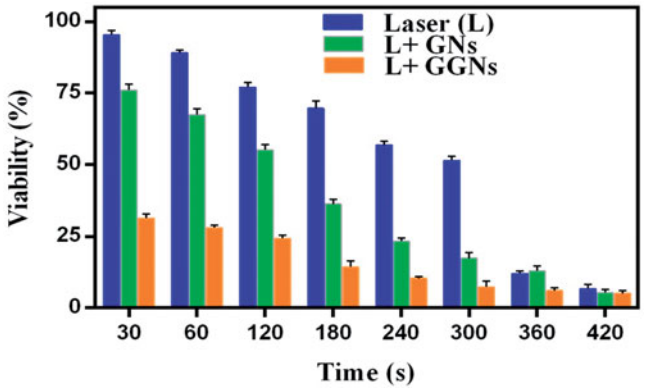

Figure 9. Photothermal effects of GGNs under the irradiation of 808 nm NIR laser in diverse times. Cell viability of A375 cells treated with NIR laser with or without incubation with 50 μg/ml GNs and GGNs. Data are presented as means ± standard deviation.

The results indicated that PTT induced a significant apoptosis in A375 cells incubated by GGNs (72%) and the percentage of live cells dropped significantly after NIR laser irradiation compared with the control group (24%).

Discussion

The main purpose of the present paper was to design and synthesize novel gold nanoshells as a photothermal agent for melanoma cancer treatment. For this purpose, gold nanoshells with silica core were synthesized successfully. The glucosamine was conjugated to GNs with the aim of targeting melanoma cancer cells. The GNs had an absorption peak around 808 nm. Figure 5 depicts the FT-IR spectra of the silica core, GNs and GGNs. In the spectrum of silica core, the peaks at 496, 800, 957 and 1099 cm^{-1} are attributed to Si–O–Si banding. The weak peaks at 1632 and 3431 cm^{-1} are assigned to stretching and bending vibration of O–H groups. Nevertheless, the intensity of these peaks in GGNs has increased, since glucose which is a polyol has been added to the GNs. A peak at is seen 1603 cm^{-1} in GGNs which is attributed to C = O of mercaptoecanoic acid as a linker and stretching O-H banding of glucose. In GGNs spectrum, the band at 2922 cm^{-1} is associated with –SH group of mercaptoecanoic acid and C–H groups present in the chain carbon of the linker and glucose. Also, strong peaks are seen at 1087 and 1260 cm^{-1} which belongs to the C–O–C and C–OH of

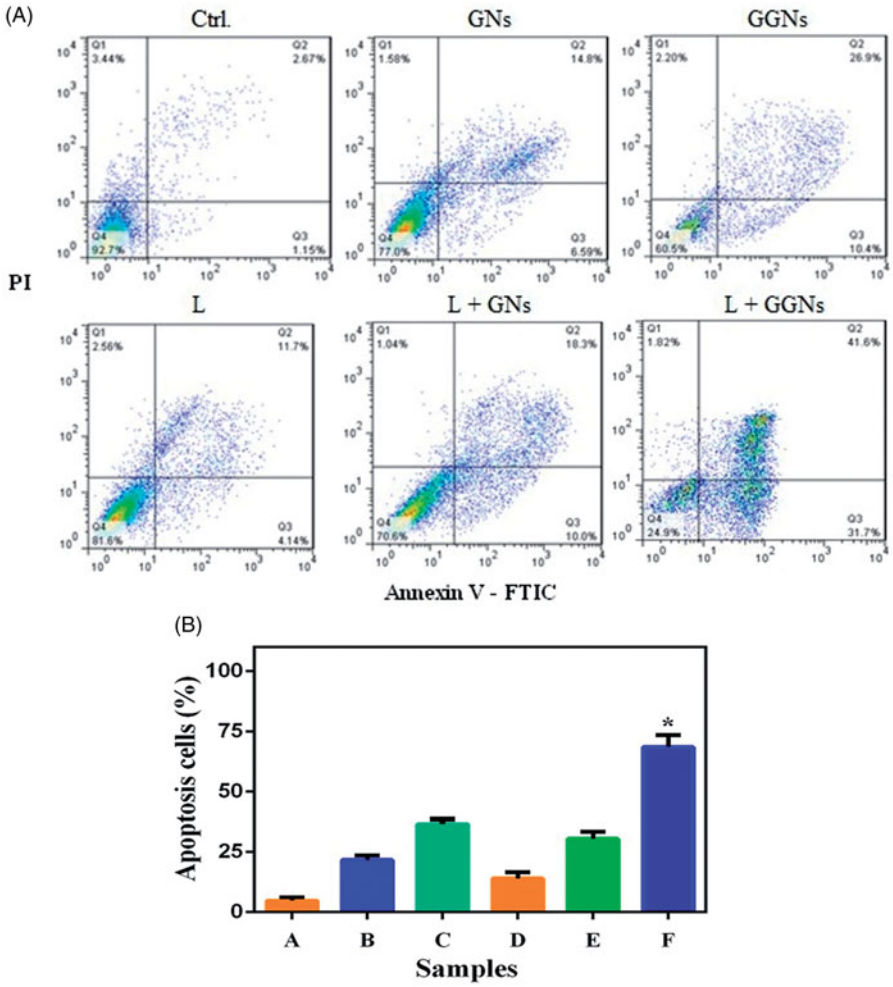

Figure 10. Flow cytometry analysis. (a) flow cytometry analysis of the A375 cells were exposed to NIR laser after incubation GNs and GGNs. (b) irradiation NIR laser in presence GGNs induce apoptosis significantly. Data are presented as the mean ± standard deviation of triplicate. *p values < 0.05, compared with apoptosis cells of control sample. A: ctrl; B: GNs; C:GGNs; D: laser; E: laser + GNs; F: laser + GGNs.

glucose. The changes which are seen at the absorption peak of GGNs in comparison with pure GNs confirm that glucose molecules have successfully attached to GNs.

The intra-cellular uptake of GGNs was measured using ICP-AES. The in-vitro studies on melanoma cells (A375) showed that the GGNs have been taken up by cells seven times more efficiently than GNs. Further, the intra-cellular uptake of GGNs in A375 cells was 25 times greater than HDF cells. This may be due to overexpression of the glucose transporter in melanoma cells in comparison with normal cells. The cytotoxicity study of melanoma cells indicates that GGNs are more cytotoxic than GNs. Although A375 cells can take up GGNs remarkably, the viability of these cells is less than that of cells treated with GNs. GGNs can be applied as a novel antitumor agent to target melanoma cells. Mehravi et al. evaluated the cellular uptake of glycosylated silica nanoprobes in human colon adenocarcinoma by flow cytometry and fluorescent microscopy. The results indicated that GSNs can be internalized into HT29 cells significantly. The high uptake of glycosylated silica nanoprobe is related to the increased demand of glucose by tumour cells [20].

The photothermal effect of GGNs was assessed using MTT assay. The viability of A375 cells exposed to 808 nm NIR laser after incubation with GNs and GGNs decreased by 64% and 29%, respectively. The data showed that the GGNs can convert the NIR energy to light energy efficiently and induce localized photothermal damage to A375 cells.

The induced apoptosis in A375 cells was measured by flow cytometry. The quantity of apoptosis in A375 cells under NIR laser irradiation after incubation with GGNs was 72%, as GGNs accumulated sufficiently in A375 cells. Therefore, the GGNs have a great targeted photothermal effect.

Anthony et al. investigated the photothermal effects of macrophage loaded with gold nanoshells on head and neck squamous cell carcinoma using MTT assay. The cells were exposed to 810 nm NIR laser with a power of 14 and 28 Wcm^{-2} for 5 and 10 min. The cells viability decreased with increased exposure time. The results indicated that 28 W/cm^2 for 10 min had the greatest cytotoxic effect [27]. Leung et al. studied the effect of the photothermal therapy using gold nanoshells and 800 nm NIR laser irradiation with a power density of 4 Wcm^{-2} for 6 and 10 min on prostate cancer cells and evaluated it using MTT assay. They found that gold nanoshells have the best cellular uptake and bring about the greatest change in cell viability under NIR laser radiation. When laser irradiation and gold nanoshells were performed together, irreversible destruction of prostate cancer cells was observed. The results approved that the gold nanoshells

have a great photothermal efficiency [28]. Wu et al. assessed the photothermal ability of conjugated GNs with anti-human CD47 monoclonal antibody in mouse ovarian cancer cells under 800 nm NIR laser irradiation for 5 min exposure using MTT assay and double-staining hochest 33342 as well as PI. Compared with all other groups, cell death was observed significantly in the group treated with GNs and NIR laser irradiation [29]. Hu et al. studied the cytotoxicity of Fe_3O_4@gold nanoshells at various concentrations on Hela cells, where dose-dependent cytotoxicity was observed. Also, the photothermal effects of the NPs were both time and concentration dependent. The results of Hela cell viability exposed to 808 nm NIR laser with a power of 15 Wcm^{-2} for different times after incubation with gold nanoshells demonstrated that photothrmal therapy of gold nanoshells was dependent on the time of exposure. Almost 50% of the Hela cells were dead after NIR laser irradiation for 5 min [30].

Conclusion

GGNs were synthesized and prepared successfully with a core-shell structure of silica@Au shell conjugated Glucosamine. Exclusive internalization into A375 cells was observed more than into HDF cells. The selective antitumor effects of GGNs on A375 cells were proved based on overexpression of transporter Glut-1. Thus, the findings confirmed that GGNs are expected to be a novel agent for killing melanoma cancer cells. Also, as suitable photothermal agents, GGNs can effectively absorb light energy and convert it to heat under NIR laser irradiation. Overall, GGNs cause irreversible damage to cancer cells compared with normal cells in-vitro. They direct cell death through apoptotic far more than necrotic the pathway. It is an important advantage of this nano-agent. These gold nanoshells are a suitable candidate for targeted chemo-photothermal therapy on melanoma cancer cells.

Acknowledgements

This study was adapted from an MSc thesis written by Samira Nouri. We thank Mr Davoodabadi for making his laser equipment available to us and Ms Sara Mayahi along with Ms Zahra Balavandi for their precious guidelines in the cell culture field, and all of the bodies that helped us to conduct this investigation.

Disclosure statement

No potential conflict of interest was reported by the authors.

Funding

We appreciate the financial support from the Research Council of Iran University of Medical Sciences.

References

[1] Chen J, Shao R, Zhang XD, et al. Applications of nanotechnology for melanoma treatment, diagnosis, and theranostics. Int J Nanomedicine. 2013;26:77–88.

[2] Zhan T, Li P, Bi B, et al. 12P-conjugated PEG-modified gold nanorods combined with near-infrared laser for tumor targeting and photothermal therapy. J Nanosci Nanotechnol. 2012;12:7198–7205.

[3] Liu Y, Xu M, Chen Q. Gold nanorods/mesoporous silica-based nanocomposite as theranostic agents for targeting near-infrared imaging and photothermal therapy induced with laser. Int J Nanomedicine. 2015;10:4747.

[4] Pemmaraju D, Appidi T, Minhas G, et al. Chlorophyll rich biomolecular fraction of *A. cadamba* loaded into polymeric nanosystem coupled with photothermal therapy: a synergistic approach for cancer theranostics. Int J Biol Macromol. 2018;110:383–391.

[5] Geng J, Sun C, Liu J, et al. Biocompatible conjugated polymer nanoparticles for efficient photothermal tumor therapy. Small. 2015;13:1603–1610.

[6] Wang C, Chen J, Talavage T. Gold nanorod/Fe_3O_4 nanoparticle "nano-pearl-necklaces" for simultaneous targeting, dual-mode imaging, and photothermal ablation of cancer cells. Angew. Chem. 2009; 121:2797–2801.

[7] Wu L, Wu M, Zeng Y, et al. Multifunctional PEG modified DOX loaded mesoporous silica nanoparticle@ CuS nanohybrids as photo-thermal agent and thermal-triggered drug release vehicle for hepatocellular carcinoma treatment. Nanotechnology. 2014;2:025102.

[8] Liu X, Fu F, Xu K, et al. Folic acid-conjugated hollow mesoporous silica/CuS nanocomposites as a difunctional nanoplatform for targeted chemo-photothermal therapy of cancer cells. J Mater Chem B. 2014;2:5358–5367.

[9] Lowery AR, Day ES, Halas NJ, et al. Immunonanoshells for targeted photothermal ablation of tumor cells. Int J Nanomedicine. 2006;1:149–154.

[10] Wang X, Liu H, Chen D, et al. Multifunctional Fe_3O_4@ P (St/MAA)@ Chitosan@ Au core/shell nanoparticles for dual imaging and photothermal therapy. ACS Appl Mater Interfaces. 2013;11:4966–4971.

[11] Hu Y, Wang R, Wang S, et al. Multifunctional Fe_3O_4@ Au core/shell nanostars: a unique platform for multimode imaging and photothermal therapy of tumors. Sci Rep. 2016;6:28325.

[12] Otis JB, Zong H, Kotylar A, et al. Dendrimer antibody conjugate to target and image HER-2 overexpressing cancer cells. Oncotarget. 2016;24:36002.

[13] Barata TS, Shaunak S, Teo T, et al. Structural studies of biologically active glycosylated polyamidoamine (PAMAM) dendrimers. J Mol Model. 2011;8:2051–2060.

[14] Carpin LB, Bickford LR, Agollah G, et al. Immunoconjugated gold nanoshell-mediated photothermal ablation of trastuzumab-resistant breast cancer cells. Breast Cancer Res Treat. 2011;125:27–34.

[15] Shen J, Li K, Cheng L, et al. Specific detection and simultaneously localized photothermal treatment of cancer cells using layer-by-layer assembled multifunctional nanoparticles. ACS Appl Mater Interfaces. 2014;6:6443–6452.

[16] Rosenholm JM, Meinander A, Peuhu E, et al. Targeting of porous hybrid silica nanoparticles to cancer cells. ACS Nano. 2009;1:197–206.

[17] Bahrami B, Mohammadnia-Afrouzi M, Bakhshaei P, et al. Folate-conjugated nanoparticles as a potent therapeutic approach in targeted cancer therapy. Tumor Biol. 2015;36:5727–5742.

[18] Mehravi B, Ahmadi M, Amanlou M, et al. N, Ghalandarlaki Conjugation of glucosamine with Gd3+-based nanoporous silica using a heterobifunctional ANB-NOS crosslinker for imaging of cancer cells. Int J Nanomedicine. 2013;8:3383.

[19] Wu TT, Zhou SH. Nanoparticle-based targeted therapeutics in head-and-neck cancer. Int J Med Sci. 2015;12:187.

[20] Mehravi B, Ahmadi M, Amanlou M, et al. Cellular uptake and imaging studies of glycosylated silica nanoprobe (GSN) in human colon adenocarcinoma (HT 29 cell line). Int J Nanomedicine. 2013;8:3209.

[21] Chattopadhyay N, Cai Z, Kwon YL, et al. Molecularly targeted gold nanoparticles enhance the radiation response of breast cancer cells and tumor xenografts to X-radiation. Breast Cancer Res Treat. 2013;1:81–91.

[22] Porta F, Lamers GEM, Morrhayim J, et al. Folic acid-modified mesoporous silica nanoparticles for cellular and nuclear targeted drug delivery. Adv Healthc Mater. 2013:2:281–286.
[23] Stöber W, Fink A, Bohn E. Controlled growth of monodisperse silica spheres in the micron size range. J Colloid Interface Sci. 1968; 26:62–69.
[24] Eptember S, Iego SAND. Uv/v/ir s a n. 2012;1–6.
[25] Manjili HK, Ma'mani L, Tavaddod S, et al. D, L-sulforaphane loaded Fe_3O_4@ gold core shell nanoparticles: a potential sulforaphane delivery system. PloS One. 2016;3:0151344.
[26] Mohammadi E, Amanlou M, Ebrahimi SE, et al. Cellular uptake, imaging and pathotoxicological studies of a novel Gd [III]–DO3A-butrol nano-formulation. Rsc Adv. 2014;86:45984–45994.
[27] Trinidad AJ, Hong SJ, Peng Q, et al. Combined concurrent photodynamic and gold nanoshell loaded macrophage-mediated photothermal therapies: an in vitro study on squamous cell head and neck carcinoma. Lasers Surg Med. 2014;46:310–318.
[28] Leung JP, Wu S, Chou LC, et al. Investigation of sub-100 nm gold nanoparticles for laser-induced thermotherapy of cancer. Nanomaterials (Basel). 2013;3:86–106.
[29] Wu CC, Yang YC, Hsu YT, et al. Nanoparticle-induced intraperitoneal hyperthermia and targeted photoablation in treating ovarian cancer. Oncotarget. 2015;29:26861.
[30] Hu R, Zheng M, Wu J, et al. Core-shell magnetic gold nanoparticles for magnetic field-enhanced radio-photothermal therapy in cervical cancer. Nanomaterials. 2017;7:111.